Ferritic-pearlitic ductile cast irons: is ΔK a useful parameter?

Francesco Iacoviello[1,*], Vittorio Di Cocco[1], Alessandra Rossi[1], Mauro Cavallini[2]

[1] Università di Cassino e del Lazio Meridionale, DICeM, via G. Di Biasio 43, 03043, Cassino (FR), Italy
[2] Università di Roma "La Sapienza", DICMA, via Eudossiana 18, Roma, Italy
* Corresponding author: iacoviello@unicas.it

Abstract In the last years, the role played by graphite nodules was deeply investigated by means of tensile and fatigue tests, performing scanning electron microscope (SEM) observations of specimens lateral surfaces during the tests ("in situ" tests). According to the experimental results, it is evident that graphite nodules damaging micromechanisms can't be merely classified as matrix nodule debonding, but depend on different parameters (e.g., loading conditions and matrix microstructure). In this work, the influence of microstructure and loading conditions on fatigue crack propagation resistance in DCIs is discussed. On the basis of experimental results, the applicability of ASTM E399 standard on the characterization of fatigue crack propagation resistance in ferritic-pearlitic DCIs is critically analyzed, mainly focusing the stress intensity factor amplitude role.

Keywords Fatigue crack propagation; Ductile cast irons; Damaging micromechanism; Stress intensity factor.

1. Introduction

In 1943, during the American Foundry Society (AFS) convention, J. W. Bolton made the following statements: *Your indulgence is requested to permit the posing of one question. Will real control of graphite shape be realized in gray iron? Visualize a material, possessing (as-cast) graphite flakes or groupings resembling those of malleable iron instead of elongated flakes* [1]. A few weeks later, in the International Nickel Company Research Laboratory, an addition of magnesium (as a copper-magnesium alloy) allowed to obtain nearly perfect spheres of graphite and, consequently, the first *ductile cast iron* (DCI), also known as nodular cast iron [2]. In 1948, always in the AFS Convention, the production of spherical graphite in iron by the addition of small amounts of cerium was announced by Henton Morrogh of the British Cast Iron Research Association. The first advantage of this production technique is evident: no high temperature/long duration heat treatments are necessary to obtain the desired shape of graphite elements (nodules), with a consequent strong cost reduction and really interesting mechanical properties: DCIs are able to combine the good castability of gray irons and the toughness of steels! In the last decades, different chemical compositions and heat treatments have been optimized in order to control the matrix microstructure and obtain different combinations of mechanical properties. Nowadays, DCIs are mainly used in the form of ductile iron pipes (for transportation of raw and tap water, sewage, slurries and process chemicals), but they are also widely used in safety related components for automotive applications (gears, bushings, suspension, brakes, steering, crankshafts) and in more critical applications as containers for storage and transportation of nuclear wastes. Matrix controls mechanical properties and matrix names are used to designate spheroidal cast iron types [3-5]. Ferritic DCI are characterized by good ductility and a tensile strength that is equivalent to a low carbon steel. Pearlitic DCIs show high strength, good wear resistance and moderate ductility. Ferritic–pearlitic grades properties are intermediate between ferritic and pearlitic ones. Martensitic ductile irons show very high strength, but low levels of toughness and ductility. Bainitic grades are characterized by a high hardness. Austenitic ductile irons show good corrosion resistance, good strength and dimensional stability at high temperature. Austempered grades show a very high wear resistance and fatigue strength.
Focusing the graphite nodules, Magnesium is the most common spheroidizing element used in the DCIs production: other elements like Si, Ca and rare earths are commonly added to reduce the

reaction violence and to promote graphite nodulizing, controlling the effect of impurities on nodules morphology and the matrix microstructure [6]. Different graphite elements nucleation theories are proposed in literature, mainly based on “heterogeneous mechanisms” (e.g. gas bubble theory, graphite theory, silicon carbide theory etc.) [7], and also different graphite nodules growth mechanisms are proposed [8]. The results obtained by other authors [9-11] by means of nanoindentation tests and by means of Micro Raman Spectroscopy and Electron Probe Microanalysis confirms the presence of a substructure in graphite nodules and of a gradient of mechanical properties, with cementite plates/particles that are trapped in and around the spherulite and multicomponent particles of Mg, Fe, S, C, etc. that are trapped in the spherulite or accumulate on the edges of the spherulite upon solidification. It is worth to note that, although the graphite tensile resistance is not negligible if compared to ferrite, it is its compression strength is absolutely not negligible, with compression resistance values that can be even 200 MPa [12, 13].
Fatigue crack propagation resistance in DCI is usually investigated according to ASTM E647 [14], analyzing the evolution of the crack growth rate (da/dN) with the increase of the stress intensity factor amplitude (ΔK), [15-19]. Considering that DCIs are characterized by a substantially composite microstructure, with graphite nodules that are a consistent volume fraction (usually about 10-15 %), the material homogeneity condition can be considered as critical in order to apply Linear Elastic Fracture Mechanics principles, and use the stress intensity factor range (ΔK) in order to characterize the stress conditions at the crack tip. In this work the fatigue crack propagation resistance of a three different ferritic-pearlitic DCI has been re-analyzed [19, 20].

2. DCIs fatigue crack propagation: Materials and tests results analysis

The investigated ferritic-pearlitic DCIs were obtained by means of chemical composition control: as a results, investigated matrix microstructures ranged from a completely ferritic DCI up to a completely pearlitic one (Figures 1-3). Chemical compositions and phases volume fractions are in Tab. 1-3.

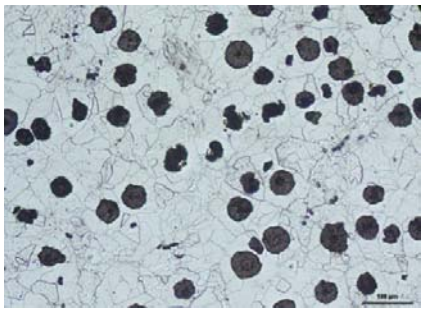

Figure 1. DCI EN GJS350-22 microstructure (100% ferrite).

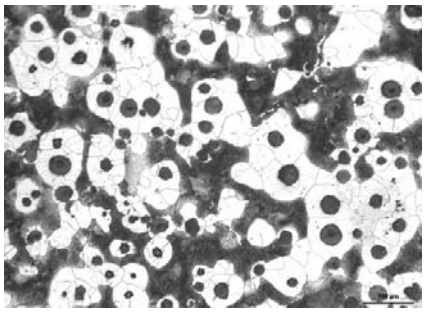

Figure 2. DCI EN GJS500-7 microstructure (50% ferrite – 50% pearlite).

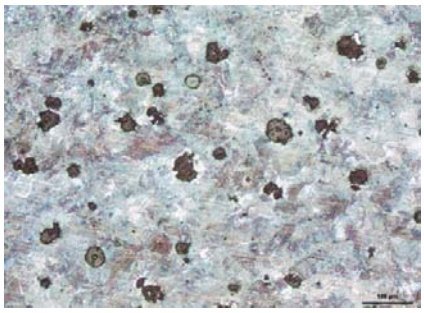

Figure 3. DCI EN GJS700-2 microstructure (100% pearlite).

Table 1. DCI EN GJS350-22 chemical composition (100% ferrite).

C	Si	Mn	S	P	Cu	Cr	Mg	Sn
3.66	2.72	0.18	0.013	0.021	0.022	0.028	0.043	0.010

Table 2. DCI EN GJS500-7 chemical composition (50% ferrite – 50% pearlite).

C	Si	Mn	S	P	Cu	Cr	Mg	Sn
3.65	2.72	0.18	0.010	0.03	-	0.05	0.055	0.035

Table 3. DCI EN GJS700-2 chemical composition (100% pearlite).

C	Si	Mn	S	P	Cu	Mo	Ni	Cr	Mg	Sn
3.59	2.65	0.19	0.012	0.028	0.04	0.004	0.029	0.061	0.060	0.098

Fatigue crack propagation tests were performed in laboratory conditions according to ASTM E647 standard [14], using 10 mm thick CT (Compact Type) specimens and considering three different stress ratio values (e.g. $R=P_{min}/P_{max}$ = 0.1; 0.5; 0.75). Tests were performed using a computer controlled servohydraulic machine in constant load amplitude conditions, considering a 20 Hz loading frequency, a sinusoidal loading waveform. Crack length measurements were performed by means of a compliance method using a double cantilever mouth gage and controlled using an optical microscope (x40).

In order to investigate the fatigue crack propagation micromechanisms, in [19, 20] the following procedures were applied:

- Scanning electron microscope (SEM) observations of the crack path during fatigue crack propagation test (cracks propagate from left to right);
- "Traditional" SEM fracture surface analysis (cracks propagate from left to right);
- 3D fracture surface reconstruction performed after SEM analysis;
- Light optical microscope (LOM) transversal crack paths analysis.

Microstructure and stress ratio influence on fatigue crack propagation resistance in ferritic-pearlitic DCIs is summarized in Figure 4.

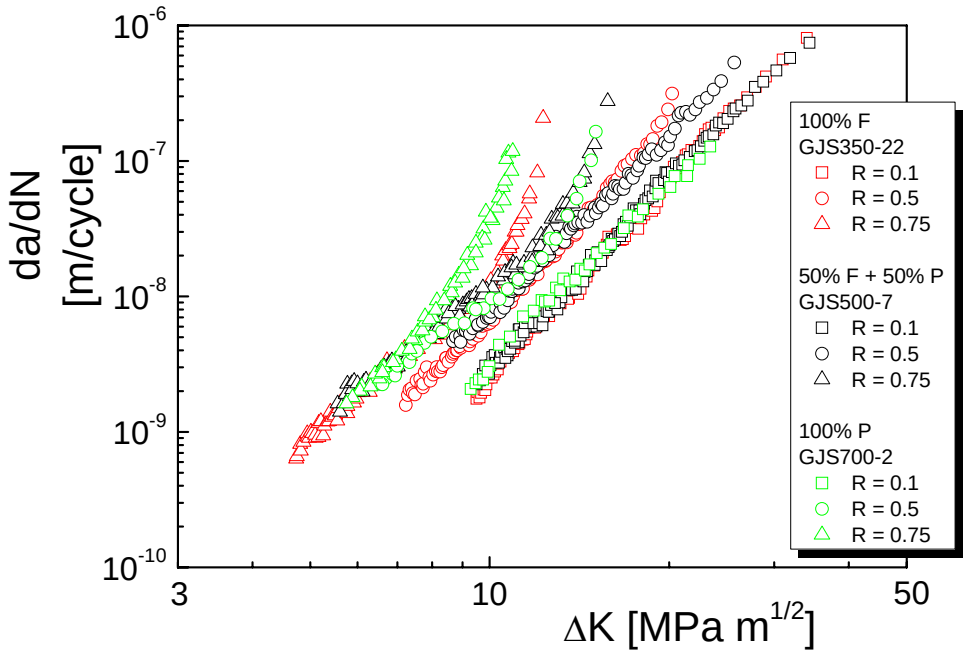

Figure 4. Loading conditions influence on fatigue crack propagation in ferritic-pearlitic DCIs.

3. LEFM considerations

Considering the linear elastic fracture mechanics principles, stress intensity factor "K" is used to quantify the stress state ("stress intensity") near the crack tip caused by a remote load or residual

stresses and, considering fatigue crack propagation, stress intensity factor range (e.g. $\Delta K = K_{max}-K_{min}$) is the main parameter used to characterize the stress conditions at the crack tip. Both K and ΔK usefulness is confirmed only considering an homogeneous and linear-elastic body: obviously, a crack tip plastic zone is always present, but, if its radius is negligible, the K parameter is still valid. Under monotonic loading, plastic zone size is usually estimated as follows:

$$r_y = \frac{1}{2\pi}\left(\frac{K}{\sigma_y}\right)^2 \quad \text{(plane stress conditions)} \tag{1}$$

$$r_y = \frac{1}{6\pi}\left(\frac{K}{\sigma_y}\right)^2 \quad \text{(plane strain conditions)} \tag{2}$$

Considering, as a first approximation, the investigated DCIs as homogeneous materials, the plastic zones size corresponding to the K_{max} value under plane strain conditions ($r_{pzK_{max}}$), calculated for the first and the last measured ΔK values (ΔK_1 and ΔK_2 respectively], can be summarized in Table 4, 5 and 6 (σ_y are considered equal to 220, 320 and 430 MPa, for the ferritic, ferritic-pearlitic and pearlitic investigated DCIs respectively). It is necessary to underline that the considered ΔK_1 and ΔK_2 are not the ΔK values corresponding respectively to the threshold and final fracture conditions, but they only can be considered as a first evaluation.

Table 4. DCI EN GJS350-22: evaluation of the plastic zone size (plane strain conditions).

R (K_{min}/K_{max})	ΔK_1 [MPa√m]	$r_{pzK_{max}}$ [mm]	ΔK_2 [MPa√m]	$r_{pzK_{max}}$ [mm]
0.1	9	0.109	32	1.368
0.5	7	0.214	20	1.754
0.75	4.5	0.355	11	2.120

Table 5. DCI EN GJS500-7: evaluation of the plastic zone size (plane strain conditions).

R (K_{min}/K_{max})	ΔK_1 [MPa√m]	$r_{pzK_{max}}$ [mm]	ΔK_2 [MPa√m]	$r_{pzK_{max}}$ [mm]
0.1	9	0.052	32	0.655
0.5	8	0.133	27	1.511
0.75	5	0.207	14	1.625

Table 6. DCI EN GJS700-2: evaluation of the plastic zone size (plane strain conditions).

R (K_{min}/K_{max})	ΔK_1 [MPa√m]	$r_{pzK_{max}}$ [mm]	ΔK_2 [MPa√m]	$r_{pzK_{max}}$ [mm]
0.1	9	0.030	22	0.179
0.5	6	0.040	13	0.203
0.75	5.5	0.145	10	0.481

Considering Figures 1-3, graphite nodules maximum diameters (d_{max}) in the investigated DCIs are respectively equal to:

- about 60-70 μm for DCI EN GJS350-22;
- about 40-50 μm for DCI EN GJS500-7 (but it is necessary to remember that nodules are surrounded by ferritic shields that are sometimes interconnected, up to 300 μm of diameter, Figure 2);
- about 45-55 μm for DCI EN GJS700-2.

Comparing d_{max} and $r_{pzK_{max}}$ values, considering that the graphite volume fraction is not negligible

(usually about 10-15%) and considering that fatigue crack propagation is characterized by the presence of a "reversed" or "cyclic" plastic zone, r_{rpz} (four times lower than the monotonic value corresponding to K_{max}) and that the tensile load reduction from the σ_{max}, and the presence of the surrounding elastic body, implies a compression condition at the crack tip, it is evident that for lower applied ΔK and/or R values:
- it is quite difficult to consider ferritic-pearlitic DCIs as homogeneous material;
- compression stress conditions are completely developed in the graphite elements at the crack tip.
Furthermore, it is necessary to remember that ferritic-pearlitic DCIs microstructure components are characterized by different mechanical properties:
- σ_Y of ferrite depends on the grain diameter, but can be assumed between 180 and 320 MPa [21].
- σ_Y of pearlite depends on the lamellae spacing, but can be assumed between to 400 and 800 MPa [21].
- graphite tensile strength is quite low (25 – 30 MPa, max [22]), but it's compression resistance is higher (even 200 MPa [23]).
On the basis of these considerations, the influence of the graphite nodules on the fatigue crack propagation should be dependent on the microstructure:
- ferritic matrix: for lower R and ΔK values the homogeneity condition is not respected; considering the r_{rpz}, it is evident that for all the investigated R values, for lower nominal ΔK values, the compression stress state is almost completely developed in the graphite nodules. Corresponding to higher ΔK values the homogeneity condition can be considered as respected, but the crack tip plastic zone can't be considered negligible (especially in plane stress conditions).
- pearlitic matrix: for all the investigated loading conditions the homogeneity condition is not respected, with d_{max} values comparable with $r_{pzK_{max}}$ values (with the exception of the higher nominal ΔK and R values); furthermore, for almost all the investigated loading conditions, the compression stress state in the reversed plastic zone is completely developed in the graphite nodules.
- ferritic-pearlitic matrix: considering the bulls eye structure of ferrite around the nodules, and the different mechanical behaviour of ferrite and pearlite, corresponding to lower nominal ΔK values, the homogeneity condition is not respected. Focusing the reversed plastic zone, corresponding to the lower ΔK values, r_{rpz} values are comparable to d_{max} values, with the compression state that is developed inside the graphite nodules. Considering the ferritic grains around the graphite nodules, the problem of the material homogeneity is evident also for ΔK values in the Paris stage.

4. Fatigue crack propagation micromechanisms

In this section, on the basis of the considerations of Section 3, and considering results already published in [19, 20], fatigue crack propagation micromechanisms in ferritic-pearlitic DCIs are re-analyzed.
Considering the ferritic DCI, the main interactions between the fatigue crack and the graphite nodule are shown in Figure 5 and 6. For lower nominal ΔK values ($r_{pzK_{max}}$ and r_{rpz} values are comparable to d_{max} values) the compression state is completely developed in the graphite nodules and secondary cracks initiate and propagate inside the nodules, with a sort of "onion-like" morphology (Figure 5). The increase of the applied ΔK implies a modification of the interaction

between graphite nodules and ferritic matrix, with the graphite nodule - ferritic matrix debonding as the main damaging micromechanism.

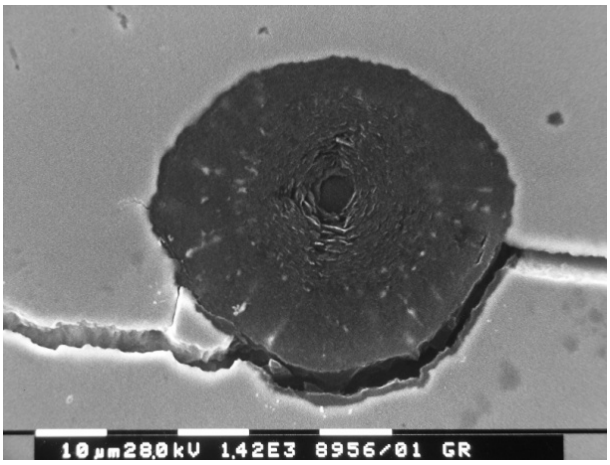

Figure 5. DCI EN GJS350-22 fatigue crack path. SEM observation of the specimen lateral surface (R = 0.1, ΔK = 10 MPa√m).

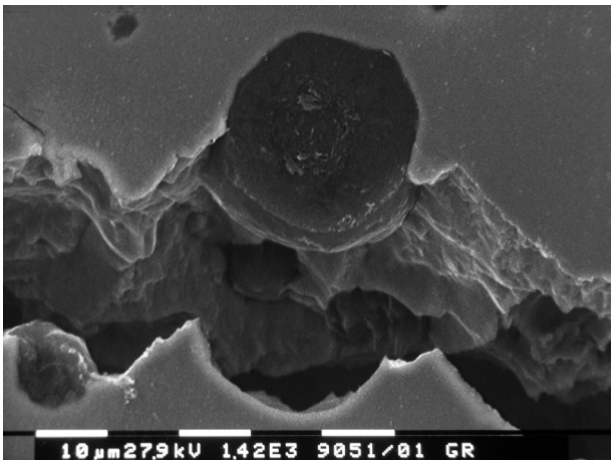

Figure 6. DCI EN GJS350-22 fatigue crack path. SEM observation of the specimen lateral surface (R = 0.1, ΔK = 22 MPa√m).

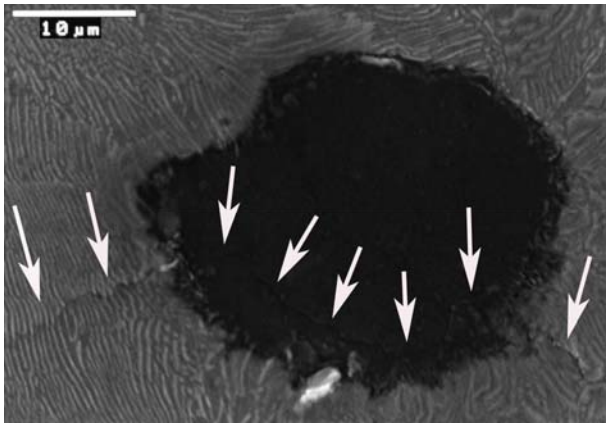

Figure 7. DCI EN GJS700-2 fatigue crack path. SEM observation of the specimen lateral surface (R = 0.1, ΔK = 22 MPa√m).

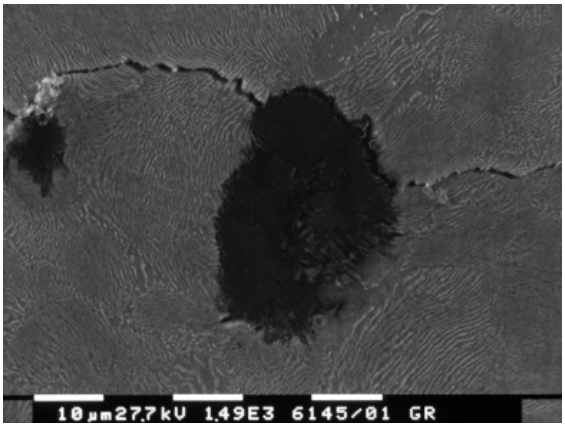

Figure 8. DCI EN GJS700-2 fatigue crack path. SEM observation of the specimen lateral surface (R = 0.5, ΔK = 10 MPa√m).

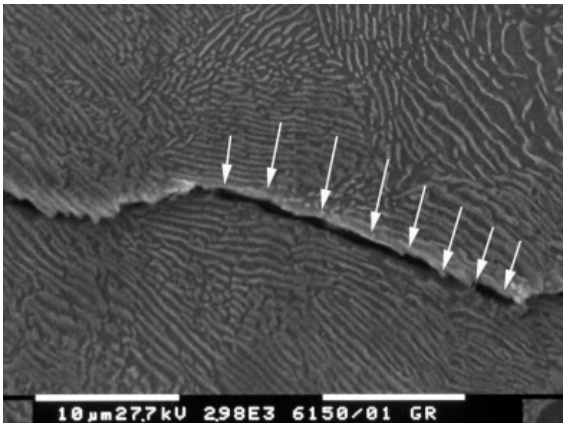

Figure 9. DCI EN GJS700-2 fatigue crack path. SEM observation of the specimen lateral surface (R = 0.75, ΔK = 7 MPa√m).

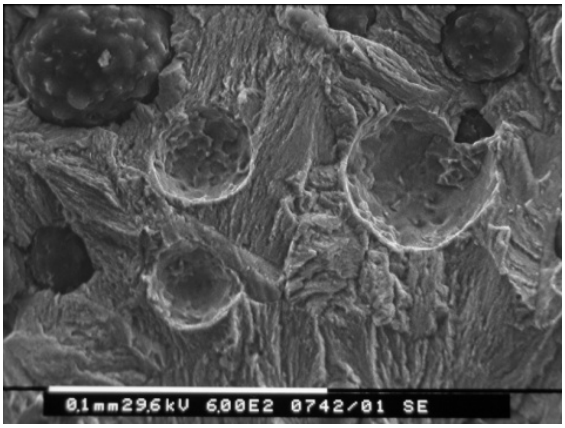

Figure 10. DCI EN GJS700-2, SEM fracture surface analysis (R = 0.1, ΔK = 16 MPa√m).

Focusing on the pearlitic DCI, the "onion like" mechanism is observed often also for higher ΔK values (Figure 7; arrows inside the graphite nodule). If the crack meets the nodule "tangentially", matrix – graphite debonding is also observed (Figure 8).
It is worth to note that the interaction between the pearlite lamellae and the fatigue crack depends on their reciprocal orientation: in fact, in Figure 7 (arrows in the matrix) the pearlitic lamellae are almost orthogonal to the crack path, with a consequent "transgranular" crack: performing a traditional SEM observation of the crack surface, these cracked lamellae have a morphology that is analogous to fatigue striations (Figure 10). If pearlitic lamellae are almost parallel to the crack path, ferrite is the preferential propagation path (arrows in Figure 7), and a traditional SEM observation of the crack surface shows a sort of cleavage.
The analysis of the microstructure influence on fatigue crack propagation in a ferritic-pearlitic DCI (with "bulls eye" microstructure morphology) is complicated by the phases distribution in the metal matrix. For all the investigated R values, considering lower ΔK values, r_{rpz} values (always calculated considering the investigated DCI as a homogeneous material) are always comparable to d_{max} values. For higher ΔK values, the graphite nodules presence is less critical. Ferritic zones around the graphite nodules are comparable to the r_{rpz} values also for the higher ΔK values. Considering the different tensile mechanical behavior of ferrite and pearlite, during fatigue loading, with K that ranges between K_{max} and K_{min}, deformation level in the involved microstructure components (ferrite and pearlite) is quite different:

- For higher K values (nearby K_{max}), plastic deformation level in ferritic shields is higher than in pearlitic matrix, due to the higher ferrite ductility;
- For lower K values (nearby K_{min}), pearlitic matrix induces a compression stress state on ferritic shields and, consequently, on graphite nodules, with an increase of crack closure effect importance. The superposition of this mechanism to the compression stress state due to the reversed plastic zone is more and more evident with the increase of ΔK and R values, with a consequent increase of the fatigue crack propagation resistance (as observed in Figure 4).

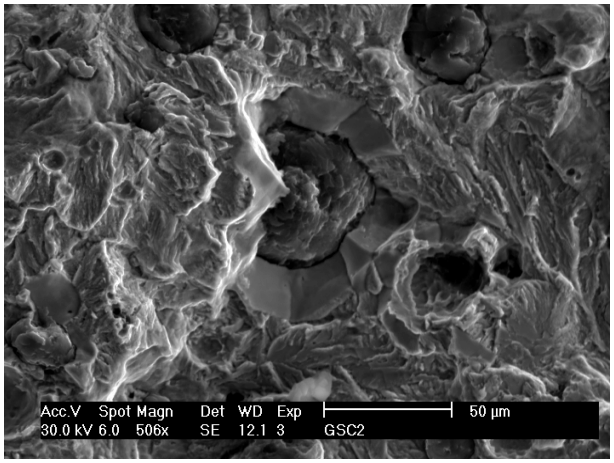

Figure 10. DCI EN GJS500-7, SEM fracture surface analysis (R = 0.1, ΔK = 15 MPa√m).

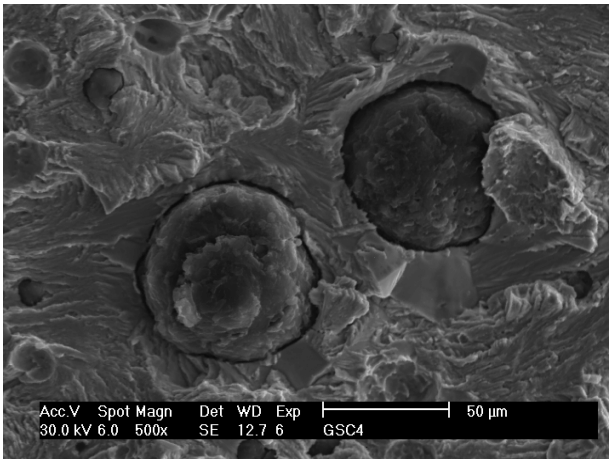

Figure 11. DCI EN GJS500-7, SEM fracture surface analysis (R = 0.75, ΔK = 8 MPa√m).

Ferritic-pearlitic DCI fracture surfaces are characterized by the presence of cleavage in ferritic shields around the graphite nodules (Figures 10 and 11) and, analogously to the pearlitic, "striations" are manly due to a "transgranular" damaging mechanism of pearlitic lamellae. All the

possible interactions between fatigue crack and graphite nodules are observed, probably due to the crack propagation direction with respect to the nodule position and to the graphite element nodularity:

- graphite nodule – matrix debonding (probably more frequent);
- onion like mechanism;
- fracture inside the graphite nodules.

5. Conclusions

Fatigue crack propagation resistance in DCI is usually investigated according to ASTM E647, investigating the evolution of the crack growth rate (da/dN) with the increase of the stress intensity factor amplitude (ΔK). Considering that DCIs are characterized by a substantially composite microstructure, with graphite nodules that are a consistent volume fraction (usually about 10-15 %), and considering the different mechanical behavior of the microstructure components, the material homogeneity condition can be considered as critical in order to apply Linear Elastic Fracture Mechanics principles.

In this work, the fatigue crack propagation resistance of a three different ferritic-pearlitic DCI has been re-analyzed, investigating the crack propagation micromechanisms and reconsidering the stress intensity factor range (ΔK) ability to characterize the stress conditions at the crack tip.

According to the observed crack propagation micromechanisms and to LEFM considerations it is possible to summarize as follows:

- Ferritic DCI: considering lower nominal ΔK and R values, $r_{pzK_{max}}$ and r_{rpz} values that are comparable to maximum values of the graphite elements diameter; as a consequence the material homogeneity condition is not respected.
- Pearlitic DCI: $r_{pzK_{max}}$ and r_{rpz} values that are comparable to maximum values of the graphite elements diameter for almost all the investigated loading conditions; as a consequence the material homogeneity condition is not confirmed.
- Ferritic-pearlitic DCI (with “bulls eye” microstructure morphology): for all the investigated R values, considering lower ΔK values, r_{rpz} values are always comparable to the graphite elements diameter. Corresponding to higher ΔK values, the graphite nodules presence is less critical; however, ferritic zones around the graphite nodules comparable to the r_{rpz} values also for the higher ΔK values.

As a consequence of this analysis, it is possible to conclude that, in order to analyze the fatigue crack propagation resistance of ferritic-pearlitic DCIs, stress intensity factor range ΔK is not able to describe the effective stress state at the crack tip for all the investigated conditions and it should be considered only a first approximation of the stress state based on the wrong hypothesis of a homogenous material.

6. References

[1] http://www.ductile.org/didata/Section2/2intro.htm
[2] D. K. Millis, P. A. Gagnebin, B. N. Pilling, Cast Ferrous Alloy, US patent 2485760, issued 1949-10-25.
[3] L.R. Jeckins, R.D. Forrest, Properties and selection: iron, steels and high performance alloys. ASM Handbook Ductile Iron, Metal Park (OH) ASM International, 1 (1993) 35-55.
[4] R.G. Ward, An Introduction to the Physical Chemistry of Iron and Steel Making. Arnold, London, 1962.

[5] C. Labrecque, M. Gagne. Review ductile iron: fifty years of continuous development. Can. Metall. Quart., 37 (1998) 343-378.
[6] T. Skaland, Ø. Grong, T. Grong. A model for the graphite formation in Ductile Cast Iron: Part I. Inoculation Mechanisms. Metallurgical Transactions A. 24A (1993) 2321-2345
[7] T. Skaland, Nucleation mechanisms in ductile iron (2005). Proceedings of the AFS Cast Iron Inoculation Conference, Schaumburg, Illinois, USA.
[8] D. M. Stefanescu. Solidification and modeling of cast iron—A short history of the defining moments, Materials Science and Engineering A, 413–414 (2005) 322–333.
[9] S. K.Pradhan, B. B.Nayak, B. K. Mohapatra, B. K. Mishra. Micro Raman spectroscopy and Electron Probe Microanalysis of graphite spherulites and flakes in cast irons. Metallurgical and materials transactions A. 38A (2007) 2363-2370.
[10] S. K. Pradhan, B. B. Nayak, S. S. Sahay, B. K. Mishra. Mechanical properties of graphite flakes and spherulites measured by nanoindentation. Carbon. 47 (2009) 2290-2299.
[11] N. X. Randall, M. Vandamme, F.-J. Ulm. Nanoindentation analysis as a two-dimensional tool for mapping the mechanical properties of complex surfaces. J. Mater. Res.. 24(3) (2009) 679-690.
[12] Union Carbide Corporation. Research and Development on Advanced Graphite Materials - Process development for graphite materials (1964). Technical Report No. WADD TR 61-72, - Air Force Materials Laboratory, Union Carbide Corporation, 35.
[13] http://www.azom.com, The A to Z of Materials.
[14] ASTM E647 – 11, Standard Test Method for Measurement of Fatigue Crack Growth Rates.
[15] K. Tokaji, T. Ogawa, K. Shamoto, Fatigue crack propagation in spheroidal graphite cast irons with different microstructure, Fatigue, 16 (1994) 344-350.
[16] G.L. Greno, J.L. Otegui, R.E. Boeri, Mechanisms of fatigue crack growth in Austempered Ductile Iron, Int. J. fo Fatigue, 21 (1999) 35-43.
[17] J. Yang, S.K. Putatunda, Near threshold fatigue crack growth behaviou of austempered ductile cast iron (ADI) processed by a novel two-step austempering process, Material Science and Engineering A, 393 (2005) 254-268.
[18] T. Mottitschka, G. Pusch, H. Biermann, L. Zybell, M. Kuna, Fatigue crack growth in nodular cast iron - Influences of graphite spherical size and variable amplitude loading, Journal of Physics: Conference Series 240 (2010) 012060.
[19] M. Cavallini, O. Di Bartolomeo, F. Iacoviello. Fatigue crack propagation damaging micromechanisms in ductile cast irons. Engineering Fracture Mechanics, 75 (2008) 694-704.
[20] F. Iacoviello, V. Di Cocco, M. Cavallini, Ductile cast irons: microstructure influence on fatigue crack propagation resistance. Frattura ed Integrità Strutturale, 13 (2010), 3-16.
[21] Metals Handbook Desk Edition, Second Edition, J.R. Davis, Editor, (1998) 153-173.
[22] Union Carbide Corporation. Research and Development on Advanced Graphite Materials - Process development for graphite materials. Technical Report No. WADD TR 61-72, - Air Force Materials Laboratory, Union Carbide Corporation, 35 (1964).
[23] http://www.azom.com, The A to Z of Materials.